One-dimensional Consolidation and Creep Characteristics of Silt in the Qinghai Lake Area

Jianzheng Liu[1], Xiaoliang Lian[2, 3], Kun Yang[1], Chunhui Wang[4], Lei Zhang[5*], Lian Chen[5]

[1] China Railway Fifth Bureau Group Co. Ltd., Guiyang, 550003, China;
[2] The 23RDMetallurgical Construction Group Co. Ltd. of Minmetals, Changsha, 410014, China;
[3] Qinghai Minmetals China Railway Highway Construction Management Co., Ltd., Xining, 810008, China;
[4] Qinghai Transportation Planning and Design Institute Co. Ltd., Xining, 81000, China;
[5] Faculty of Civil Engineering and Mechanics, Kunming University of Science and Technology, Kunming, 650500, China.
zl5359@163.com

Abstract. The prediction of post-construction consolidation and settlement is critical for assessing the deformation of a soft soil subgrade. One-dimensional consolidation creep test was conducted to analyze the creep characteristics of a soft silt subgrade of a highway constructed near Qinghai Lake. The test results showed the following. The stress-strain curve of the silt was nonlinear. The higher the stress, the sooner the soil entered the secondary consolidation stage. The transition between the primary and secondary consolidation stages occurred at 100 min. The generalized Kelvin model, Burgers model, Singh-Mitchell model, and power function empirical model were selected to fit the experimental results and obtain the model parameters. The Singh-Mitchell and the power function empirical model provided the best performances for reflecting the creep characteristics of the Qinghai Lake silt. Thus, these models can be used to estimate the post-construction settlement and deformation of this soil type.

Key words: Silts; creep characteristics; deformation; laboratory tests; creep model;

1 Introduction

Soil creep refers to the phenomenon that the deformation of soil increases with time. This process significantly affects engineering projects. Several soil creep models have been proposed recently, such as empirical model, component model. Adachi and Oka [1] established creep models based on the Cam-Clay yield model, and the modified Cam-Clay model proposed by Roscoe and Burland, respectively. Jiang et al. [2] used different models to predict different types of soil deformation under different working

W. Guo et al. (eds.), *Proceedings of the 3rd International Conference on Green Building, Civil Engineering and Smart City (GBCESC 2024)*, Advances in Engineering Research 264,
https://doi.org/10.2991/978-94-6463-728-1_42

conditions. Zhou et al. [3] conducted one-dimensional consolidation creep tests to assess the creep characteristics of different soil types and established creep models or creep equations.

The literature review shows that most studies use consolidation creep test results and creep models to predict the deformation characteristics of soil.

This study performs a one-dimensional consolidation creep test to determine the creep characteristics of typical silt soil in the Qinghai Lake region. Suitable creep models are selected to describe the creep characteristics of the silt. The predicted and experimental results are compared to determine the optimal creep model to reflect the creep characteristics of the Qinghai Lake silt soil.

2 One-dimensional consolidation test

2.1 Soil sampling

The silt used in the test was obtained from a highway project site near the Chahanuo village, Wulan County, Haixi Prefecture, Qinghai Province. The sampling location is shown in Fig. 1.

Fig. 1. Sampling location[8]

The main landforms at the sampling site are river valleys and low mountains. The outcrop stratum dates from the Quaternary in the Holocene epoch. The soil layer is brownish-gray, soft, plastic silt and chalky clay, with a thickness of 5-12 m. It is high compressibility and high-water content. The road section passing through the construction road has serious water accumulation. From June to August, the water accumulation can reach 10 ~ 20 cm, the water grass (plateau meadow) is rich, and the grass height is 30 ~ 40 cm. The physical and mechanical properties of the powdered soil are listed in Table 1.

Table 1. Indicators of physical and mechanical properties of the Qinghai Lake silt

Natural density ρ (g/cm³)	Water content w (%)	Compression modulus E (MPa)	Cohesive force *c* (kPa)	Internal friction angle φ (°)	Liquid limit W_L (%)	Plastic limit W_P (%)
1.91	37.1	4.8	9	16	45	20

2.2 Test methods

Fig. 2. Model WG consolidation meter(photographed by the author)

Fig. 3. Specimen preparation(photographed by the author)

A Model WG consolidation meter was used in the one-dimensional consolidation creep tests (Figure 2). The three specimens (6.18 cm diameter and 2 cm height) were obtained with a ring knife and were prepared following the standard for geotechnical test methods [5].

The selection of appropriate stability standards is not only related to the difficulty of conducting the experiment, but also to the accuracy of the experiment. Currently, there is no clear standard to indicate the stability standard for creep. However, the standard for achieving creep stability is usually the deformation of soil samples within 24 hours, which is less than 0.01mm [9].

In order to determine the creep stability standard of typical silt in Qinghai Lake, saturated silt samples are now loaded and the changes in soil creep are observed to determine the stability standard. Conduct one-dimensional consolidation creep tests on 6 sets of saturated silt samples, using the same method as the one-dimensional consolidation creep test described below. Apply a load of 200kPa and record data every 1440 minutes (24 hours). The test data record table is shown in Table 2:

Table 2. The deformation stability test data

Sample number / Time (min)	1	2	3	4	5	6
1440	213.4	242.6	235.2	232.2	218.6	228.7
2880	214.5	243.5	236.2	233.2	219.8	230
4320	215.4	244.3	237.2	234.8	221.4	231.2
5760	216.8	245.2	238.2	235.8	222.2	231.9
7200	217.2	246.0	238.5	236.1	222.9	232.5
8640	217.3	246.3	238.8	236.5	223.2	232.8
10080	217.3	246.4	239.0	236.7	223.2	232.9

In summary, this article takes the deformation of the sample within 1440 minutes (24 hours) not exceeding 0.01mm as the stability standard for the one-dimensional consolidation creep test of typical silt in Qinghai Lake. The sample should be loaded for at least 7200 minutes, and if the deformation does not exceed 0.01mm within 1440 minutes (24 hours) after exceeding 7200 minutes, the stability standard should be continued until it is reached before the next level of load can be applied.

The specimens were saturated by placing them into a vacuum saturation device (Fig. 3). Double-sided drainage and graded loading were used during the test. The saturated specimens were placed into the consolidation device, and the loading sequence was 12.5 kPa→25 kPa→50 kPa→100kPa→200 kPa→400 kPa→800 kPa. After the first loading, filled the sink with water. Counted at 6 s, 12 s, 1 min, 2 min 15 s, 4 min, 6 min 15 s, 9 min, 12 min 15 s, 16 min, 20 min 15 s, 25 min, 30 min 15 s, 36 min, 49 min, 64 min, 100 min, 200 min, 400 min, 1380 min, 1440 min, 2880 min, 4320 min, 5760 min, and 7200 min. Until the deformation was stable. The deformation stability meant that the deformation of the specimen was less than 0.01 mm within 24 h under each level of load. After the deformation was stable, the next load was applied until the end of loading [5]. Since the test results of each group were similar, one group of data was taken as an example for analysis.

3 Test results

3.1 Strain-time relationship

The strain-time curves of the silt under graded loading are shown in Fig. 4.

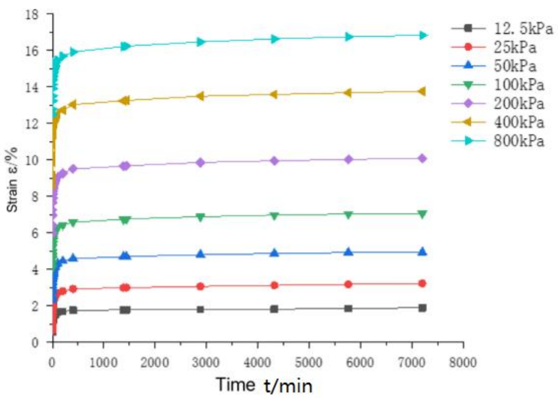

Fig. 4. Creep duration curve

The change rate of the strain is high at the beginning of the test, and the deformation increases rapidly. Subsequently, the deformation and deformation rates decrease, and the curve stabilizes. The reason is that the deformation is rapid in the initial stage due to compression deformation. As the pore water is being discharged, the deformation rate decreases. As the pore water discharge, the soil skeleton is compressed, and the deformation is very small. When the load is applied, the instantaneous settlement occurs first, followed by the main consolidation deformation and the secondary consolidation deformation. The test data show that the amount of deformation is related to the consolidation pressure. The deformation is lower, and the stabilization time is shorter at lower consolidation pressure and vice versa.

3.2 Void ratio-time relationship

The logarithmic curves of the void ratio over time for the soil specimens are shown in Fig. 5.

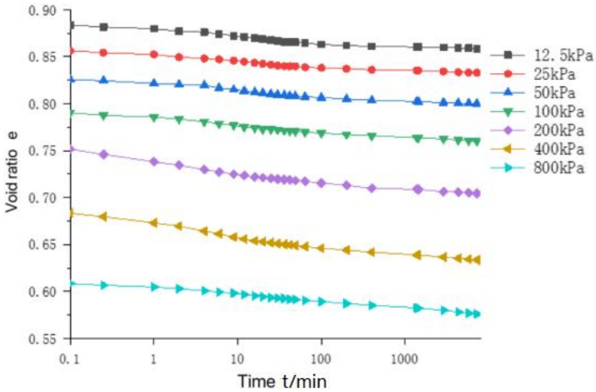

Fig. 5. Void ratio and time logarithmic curve

The void ratio changes greatly in the initial stage (0 ~ 100min) and then tends to be stable. With the increase of applied stress, the void ratio-time curve becomes gentler. It shows that the higher the consolidation pressure, the more the pore water discharged, and the faster the soil enters the secondary consolidation stage [1]. The change rate of void ratio is higher at the beginning of the test, and the deformation rate is higher. After the soil enters the secondary consolidation stage, the soil skeleton deforms, the deformation rate is low, and the change rate of the void ratio decreases.

3.3 Stress-strain relationship

The stress-strain relationship of the silt is shown in Fig. 6. The variation trend of stress-strain isochronous curve at different time is basically the same， and the stress-strain relationship is nonlinear. In the same time period, the strain increases with the consolidation stress. At the same consolidation stress, the stress increases with time. This shows that the elastic modulus of the specimen decreases with the increase of stress.

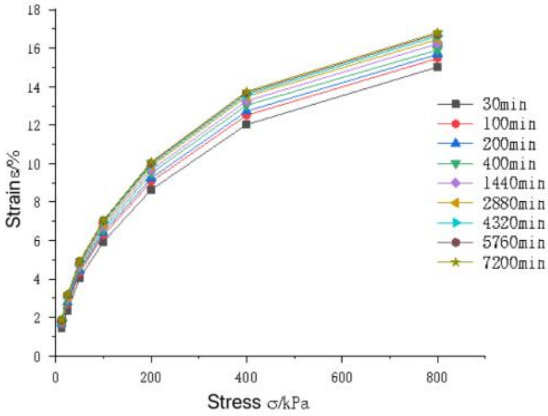

Fig. 6. Stress-strain isochronous curve

3.4 Logarithmic strain-time relationship

The double logarithmic curves of the strain-time relationship for the silt are shown in Fig.7.

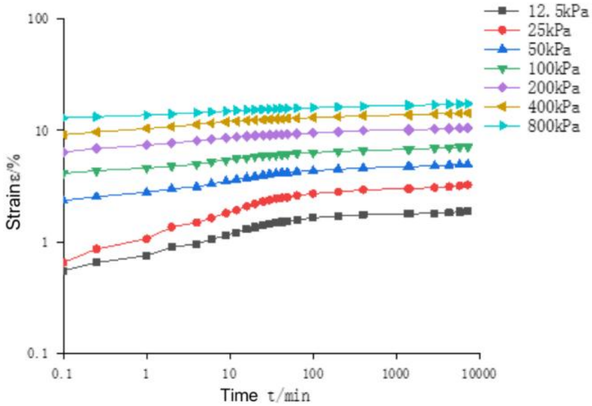

Fig. 7. Double logarithmic curves of strain-time relationship

The change trend of strain-time log curve under different stress is basically the same. At the same time, the larger the loading stress is, the larger the strain is. The rate of change in the strain-time relationship changes at 100 min. The rate of change is larger at a lower stress (12.5 kPa and 25 kPa). After 100 min, the change rate became smaller, and the change rate was the smallest at 800 kPa. At this time, the curve was close to a straight line.

4 Consolidation characteristics

4.1 Transition between primary and secondary consolidation

The Casagrande diagram method (Fig. 8) was used to determine the division point of the primary and secondary consolidation stages in the deformation process [2]. The method uses the intersection of two lines (the middle and tail of the e-log t curve of the soil) to represent the division point of the primary and secondary consolidation stages.

The division points of the primary and secondary consolidation stages under different loads are shown in Fig.9.

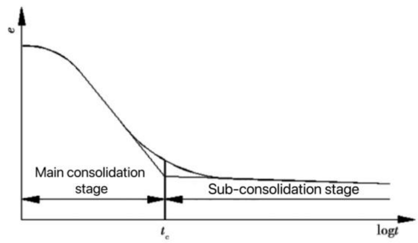

Fig. 8. The transition between the primary and secondary consolidation stages

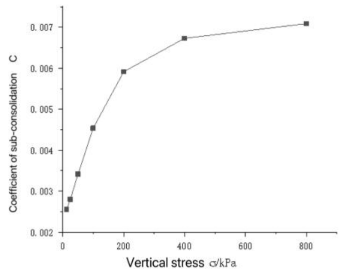

Fig. 9. Relationship curve between secondary consolidation coefficient and stress

The secondary junction coefficient increases with the increase of stress. When the vertical stress reaches 200 kPa, the increase rate decreases and the curve tends to be stable. When the vertical stress reaches 200 kPa, the consolidation pressure changes the soil structure and causes secondary consolidation deformation. The inflection points of the curve appeared at 80 ~ 200 min.

It is generally considered that the critical point of primary and secondary consolidation settlement for ideal soil is the time when excess pore water pressure dissipates and soil skeleton begins to deform. The test data and process show that the excess pore water pressure dissipation process of silty soil is very long. The dissipation of excess pore water pressure is accompanied by the deformation of soil skeleton, which makes it difficult to determine the critical point of primary and secondary consolidation settlement. Due to the limitation of space, this paper does not do too much analysis on the factors affecting the primary and secondary consolidation boundary points, only based on the Casagrande graphic method to determine.

4.2 Deformation

Based on the data in Fig. 4 and Fig. 9, 100 min is considered the division point between the primary and secondary consolidation, and 7200 min is the end of the secondary consolidation stage. The data were used to calculate the proportion of deformation in the primary and secondary consolidation stages. The results are listed in Table 3.

Table 3. Proportion of deformation of pulverized soil during different consolidation stages (300 min)

Consolidation stress (kPa)	Total settlement (mm)	Instantaneous subsidence (mm)	Primary consolidation deformation (mm)	Secondary consolidation deformation (mm)	Proportion of transient settlement (%)	Proportion of primary consolidation settlement (%)	Proportion of secondary consolidation settlement (%)	Proportion of primary consolidation / total consolidation (%)
25	0.65	0.08	0.46	0.11	13.10	70.62	16.28	81.27
50	0.99	0.30	0.56	0.13	30.67	56.53	12.80	81.54
100	1.41	0.53	0.72	0.16	37.69	51.13	11.17	82.07
200	2.09	0.83	1.06	0.21	39.61	50.60	9.79	83.79
12.5	0.38	0.07	0.26	0.05	18.92	67.86	13.23	83.69
400	2.84	1.18	1.41	0.25	41.58	49.69	8.73	85.06
800	3.45	1.68	1.50	0.27	48.61	43.54	7.86	84.72

5 Creep model

For the widely used creep models, this article will analyze and select a creep model suitable for typical silt in Qinghai Lake from two types of models: component model and empirical model.

5.1 Generalized Kelvin Model

The generalized Kelvin model [6] consists of an elastic component H in series with a Kelvin body, i.e., K = H-K. The diagram of the generalized Kelvin model is shown in Fig. 10. Eq. (1) is the one-dimensional creep equation.

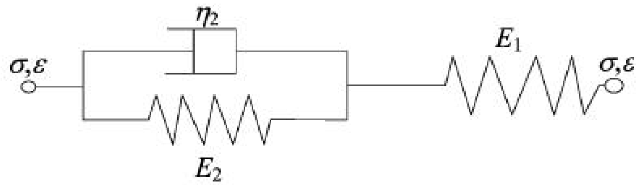

Fig. 10. Mechanical diagram of the generalized Kelvin rheological model

$$\varepsilon(t) = \frac{\sigma_0}{E_1} + \frac{\sigma_0}{E_2}\left(1 - e^{-\frac{E_2}{\eta_2}t}\right) \tag{1}$$

where $\varepsilon(t)$ is the strain at time t under a load; E_1 is the elastic modulus of the spring; η_2 and E_2 are the viscous coefficient and elastic modulus of the Kelvin body; σ_0 is the applied consolidation stress. σ_0 is a constant. There are three unknown parameters in Eq. (1).

When t = 0,

$$\varepsilon_0 = \frac{\sigma_0}{E_1} \tag{2}$$

where ε_0 is the instantaneous deformation at t = 0. The following is obtained from the test:

$$E_1 = \frac{\sigma_0}{\varepsilon_0} \tag{3}$$

Equation (1) can be transformed to obtain two unknown parameters. We established the model and fit the test data to obtain the model parameters for different normal stresses.

5.2 Burgers model

Burgers model [6] describes the creep mechanism of an elastic-viscous body. It consists of a Kelvin body in series with a Maxwell body, i.e., Bu = Mx-K. The mechanical diagram of Burger's model is shown in Fig. 11. Eq. (4) is the constant-stress creep equation.

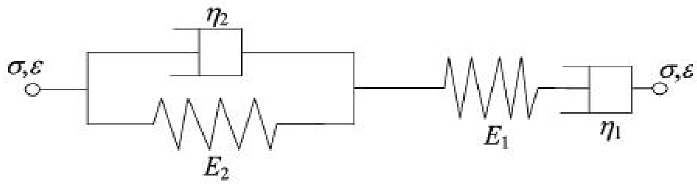

Fig. 11. Mechanical diagram of Burger's model

$$\varepsilon(t) = \frac{\sigma_0}{E_1} + \frac{\sigma_0}{\eta_1}t + \frac{\sigma_0}{E_2}\left(1 - e^{-\frac{E_2}{\eta_2}t}\right) \tag{4}$$

where $\varepsilon(t)$ is the strain at time t under a load; E_1 is the elastic modulus of the spring; η_1 is the viscous coefficient of the sticky pot; η_2 and E_2 are the viscous coefficient and elastic modulus of the Kelvin body, and σ_0 is the applied consolidation stress. There are four unknown parameters in Eq. (4).

The instantaneous deformation ε_0 at t = 0 is obtained. Similar to the procedure for the generalized Kelvin equation, E_1 is obtained using Eqs. (2), (3), and the test data. According to Eq. (5), as time t increases, the creep-time curve changes to a straight line. The slope of the line is obtained by fitting. The slope is defined as K:

$$\mathrm{K} = \frac{\sigma_0}{\eta_1} \tag{5}$$

η_1 can be obtained by fitting solution. Thus, the four unknown parameters in Eq. (4) are transformed into two unknown parameters. We established the model and fit the test data to obtain the unknown parameters.

5.3 Empirical model with a power function

Only vertical deformation occurs in the one-dimensional consolidation test because the specimen is laterally constrained. Deformation causes discharges of air and water from the soil specimen, pore compression, and changes in the structure and arrangement of the soil particles. The compressive deformation of the soil particles is negligible and was ignored. The vertical pressure is considered to be uniform [4]; thus, all elements in the soil specimen satisfy the following equation:

$$E_t = \frac{\sigma_0}{\varepsilon_t} \tag{6}$$

where σ_0——stress constant;

ε_t——deformation of the soil specimen at time t;

E_t——deformation modulus of the soil specimen at time t.

Equation (6) and the data from the one-dimensional consolidation test were used to derive a plot of σ/ε-σ. The deformation modulus over time was calculated using the following power function, and a and b were obtained:

$$E_t = \mathrm{a}t^b \tag{7}$$

where E_t——deformation modulus of the soil specimen at time t;

t——test time;

a、b——parameters of Eq(7).

5.4 Singh-Mitchell model

The Singh-Mitchell model [7,4] is an empirical model describing the creep characteristics of soils using data from a triaxial creep test. The mode is widely used in engineering and is applicable to one-dimensional consolidation test data. The Singh-Mitchell model describes the shear stress-strain relationship using an exponential function and describes the strain-time relationship using a power function. The empirical equation is defined as follows:

$$\dot{\varepsilon} = Ae^{\alpha D}\left(\frac{t_1}{t}\right)^m \tag{8}$$

w here $\dot{\varepsilon}$——the strain rate of the soil;

D——the level of shear stress, which is the vertical stress in a one-dimensional consolidation test;

t_1——unit time;

t——Time of loading during the test;

A、α、m——test constants.

When the test constant m ≠ 1, integrating Eq. (8) and collapsing gives:

$$\varepsilon = \varepsilon_0 + \frac{At_1}{1-m}e^{\alpha D}\left(\frac{t}{t_1}\right)^{1-m} \tag{9}$$

where ε_0 is the instantaneous deformation. When it is not considered, Eq. (9) can be transformed into:

$$\varepsilon = \mathrm{B}e^{\alpha D}\left(\frac{t}{t_1}\right)^{\lambda} \tag{10}$$

Where $B = \frac{At_1}{1-m}$, $\lambda = 1 - m$ is the slope λ of the stress-strain double logarithmic curve of the specimen under different load levels.

The trends of the stress-strain curves are similar at different times. A hyperbolic function is used to fit the stress-strain relationship:

$$\varepsilon = \frac{\sigma}{a + b\sigma} \tag{11}$$

where a and b are the fitted parameters.

6 Model Validation and Comparison

Due to the great discreteness of loading characteristics in geotechnical engineering, To improve the logic of the data, In the fitting, the load condition which appears frequently in engineering is adopted, To ensure the reliability of the data. In this paper, the model curves and test data under the action of 200 kPa, which often occurs in engineering, are selected as examples. The fitted curves of the Singh-Mitchell model, empirical model with a power function, generalized Kelvin model, and Burger's model were compared with the experimental data for a load of 200 kPa (Fig. 12).

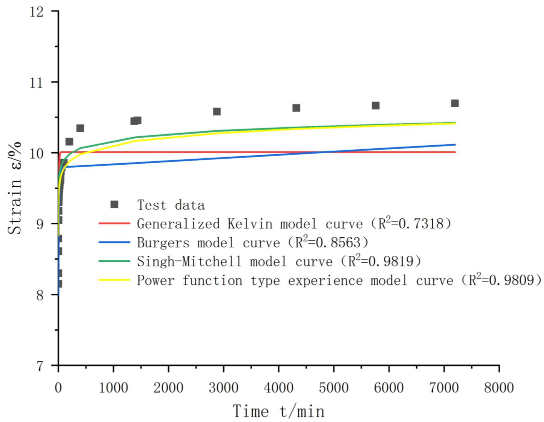

Fig. 12. Comparison of experimental data and different models under a vertical stress of 200 kPa

The trends of the four models are similar for describing the creep of the Qinghai Lake silt. However, they exhibit different levels of accuracy. The Singh-Mitchell model and the power function model are superior to the other models. The former exhibits the best fitting performance, with a correlation index (R^2) of 0.98. The generalized Kelvin model has the lowest correlation index, with an R^2 of 0.73. Therefore, the Singh-Mitchell model and the power function model are the best models to describe the post-construction deformation and creep of the Qinghai Lake silt.

7 Conclusion

One-dimensional consolidation creep tests were performed to investigate the deformation and creep characteristics of a soft silt subgrade of a highway constructed near Qinghai Lake.

(1) The stress-strain relationship of the silt was nonlinear. The deformation rate was larger at the beginning of the test and then increased over time, and the curve flattened.

(2) The division points of the primary and secondary consolidation stages were determined by the Casagrande graphic method. The dividing point is 100 min, and the deformation is about half of the total deformation. The deformation of the main consolidation stage accounts for 82-85 % of the total deformation. Therefore, the post-construction settlement is large.

(3) The fitting of generalized Kelvin model, Burgers model, Singh-Mitchell model and power function empirical model to the creep characteristics of Qinghai Lake silt is compared and analyzed. The Singh-Mitchell model and the empirical model are the most suitable models to describe the creep characteristics of silt. Therefore, these two models can be used to analyze and predict the post-construction settlement and deformation of the Qinghai Lake silt.

Data Availability

The data used to support the finding of this study are included with in the article.

Conflicts of Interest

The authors declare that they have no conflicts of interest.

Acknowledgments

This study was supported by the sub-topics of the scientific and technological achievements transformation project of Qinghai Provincial Science and Technology Department (2021-SF-168) and School of Architectural Engineering, Kunming University of Science and Technology(2022M20212110025).

The manuscript detailing contributions of each author: 1. Conceptualization: Liu Jianzheng; 2. Data Curation & Supervision: Lian Xiaoliang; 3. Investigation & Supervision: Yang Kun; 4. Methodology & Supervision: Wang Chunhui; 5. Visualization & Supervision: Zhang Lei; 6. Writing – original draft & Writing - Review & Editing: Chen Lian.

References

1. Adachi T, Oka F. Constitutive equations for normally consolidated clay based on elasto-viscoplasticity. Soils Found, 1982, 22(4): 57-70.
2. Xunli Jiang, Zhiyi Huang and Xue Luo. An Improved Mechanistic-Empirical Creep Model for Unsaturated Soft and Stabilized Soils. Materials, 2021, 14: 2-21.
3. Zhou Feng-xi, Wang Li-ye, Lai Yuan-ming. One-dimensional creep tests and model studies on saturated saline soil. Chinese Journal of Geotechnical Engineering, 2020, 42(1): 142-149.
4. Yang Aiwu, Liang Zhenzhen, Yang Shaokun. Study on the One-Dimensional Consolidation Creep Characteristics of Tianjin Binhai Remoulded Soft Clay. Chinese Journal of Underground Space and Engineering, 2022, 18(5): 1532-1538.
5. Ministry of Water Resources of the People's Republic of China, GBT50123-2019, Standard for geotechnical test methods. Beijing: China Planning Press, 2019.
6. Yu Pengcheng. Experimental study on creep properties of dredger fill. Liaoning: Dalian University of Technology, 2012.
7. Singh A, Mitchell J K. General stress-strain-time function for soils. Journal of the Soil Mechanics and Foundations Division, 1968, 94(1): 21-46.
8. Lei Z ,Jixiang Y ,Jiake T , et al.Study on the Influence of Moisture Content and Drying-Wetting Cycles on the Shear Strength Index of Silt in the West Bank of Qinghai Lake[J].Advances in Civil Engineering,2021,2021
9. Deng Zhibin. Research and application of creep test and constitutive model identification method for soft clay [D] Changsha, Central South University, 2007.